Article

Journal of
Nanoscience and Nanotechnology
Vol. 18, 188–194, 2018
www.aspbs.com/jnn

Strong Hydrogen Bonding with Inorganic Pendant Polyhedral Oligomeric Silsesquioxane Nanoparticles Provides High Glass Transition Temperature Poly(methyl methacrylate) Copolymers

Shu-Ling Yeh[1,2], Chao-Yuan Zhu[1,*], and Shiao-Wei Kuo[3,*]

[1]*Department of Applied Chemistry, National Chiao Tung University, Hsinchu, 300, Taiwan*
[2]*Material and Chemical Research Laboratories, Industrial Technology Research Institute, Hsinchu 300, Taiwan*
[3]*Department of Materials and Optoelectronic Science, National Sun Yat-Sen University, Kaohsiung 80424, Taiwan*

We report a series of poly(methyl methacrylate) (PMMA) copolymers containing small amounts of methacrylamide (MAAM) and pendant polyhedral oligomeric silsesquioxane (POSS) methyl acrylate (MAPOSS) segments. The hydrogen bonding interactions of the MAAM monomer units and the inorganic POSS nanoparticle units improved the thermal and mechanical properties of the PMMA copolymers. For example, PMMA copolymerization with 5 wt% PMAAM and 5 wt% PMAPOSS monomers could enhance the glass transition temperature to 142 °C, with higher modulus, higher water contact angle, and reasonably high transparency. Such copolymers have potential to replace PMMA homopolymers in optical applications.

Keywords: Poly(methyl methacrylate), Hydrogen Bonding, POSS, Nanoparticle.

1. INTRODUCTION

Polymers have extensive applications not only in the biomaterial industry but also in optoelectronics,[1] organic light-emitting diodes,[2] and display backlighting.[3] These optoelectronic polymers—including poly(methyl methacrylate) (PMMA), polystyrene (PS), and polycarbonate homopolymers—usually have attractive transparency, thermal processability, and the ability to be mass produced inexpensively. Among these thermoplastics, PMMA homopolymers have excellent optical properties for use as organic glass, including resistance against weathering corrosion, ready mass production at low cost, and high insulating properties. Nevertheless, PMMA homopolymers have low glass transition temperatures and high degree of moisture absorption, limiting their potential applications in the optoelectronics industry.[4–16]

The glass transition temperatures (T_g) of polymers are strongly dependent on their chemical structures and physical interactions. In previous studies,[17–21] we found that the copolymerization of strong hydrogen bonding donor or acceptor monomers can improve values of T_g as a result of the compositional heterogeneity effect.[22] Incorporating such monomers into PMMA copolymers for optoelectronic applications requires that they possess three characteristics: the hydrogen bonding donor units to increase the glass transition temperatures of the PMMA copolymers; hydrophobic units to decrease the moisture absorption of the PMMA copolymers; and non-aromatic ring structure to avoid poor transmittance in the near-UV region. Most importantly, the contents of these monomers should be very low to avoid changing the properties of the PMMA. For instance, we found that polymerizing 15 wt% methacrylamide (MAAM) and methyl methacrylate (MMA) to form PMMA-*co*-PMAAM could increase the value of T_g at 144 °C,[17] but the moisture absorption increased as well to 4.5 wt%. In contrast, the incorporation of styrene monomer (12 wt%) decreased the moisture absorption to approximately 1.0 wt% because of the hydrophobic nature of the PS segments.[18] Nevertheless, incorporating PS segments (12 wt%) into the PMMA-*co*-PMAAM copolymer decreased the value of T_g to 118 °C and led to poor transmittance in the near-UV region, limiting optoelectronic applications.[18] Accordingly, tricyclodecyl

*Authors to whom correspondence should be addressed.

 1533-4880/2018/18/188/007 doi:10.1166/jnn.2018.14570

methacrylate and isobornyl methacrylate monomers have been incorporated into PMMA-*co*-PMAAM copolymers to ensure excellent transmittance in the near-UV region.[20] Because all of the monomers used in those studies were organic compounds, they were needed in relatively high amounts to enhance the thermal properties of the PMMA copolymers while maintaining the optical properties.[17–21]

Another approach toward improving the thermal properties of PMMA is to form organic/inorganic composites by incorporating nanoparticles to form nanoarchitectonic materials.[23–25] For example, Wanke et al. reported the bulk copolymerization of the pendant polyhedral oligomeric silsesquioxane (POSS) methyl acrylate (MA-POSS) monomers and MMA and investigated the effects of different vertex groups on the thermal properties.[26] The incorporation of inorganic POSS derivatives into organic polymers has received much attention recently because the nanoscale dimensions (diameters: 1–3 nm) of these nanoparticles can impart excellent thermal and mechanical properties.[27–29]

In this study, we used bulk polymerization to synthesize a series of random copolymers of poly(methyl methacrylate-*co*-methacrylamide-*co*-methacrylate isobutyl-POSS) (PMMA-*co*-PMAAM-*co*-PMAPOSS) containing small amounts of the MAAM and MAPOSS monomer units. The incorporation of the bulk POSS monomer maintained the excellent transmittance in the near-UV region and low moisture absorption, whereas the hydrogen bonding interactions of the MAAM monomer units hindered the free rotation and, therefore, enhanced the thermal properties of the PMMA copolymers. The thermal, optical, and surface properties and specific interactions of these copolymers were analyzed using differential scanning calorimetry (DSC), thermogravimetric analysis (TGA), dynamic mechanical analysis (DMA), contact angle measurements, and Fourier transform infrared (FTIR) spectroscopy.

2. EXPERIMENTAL SECTION

2.1. Materials

MMA was purchased from Showa Chemical Industry. Benzoyl peroxide (BPO) was obtained from Evonik. MAAM was purchased from Sigma–Aldrich. Methacrylate Isobutyl-POSS was obtained from Hybrid Plastics.

The Synthesis of Poly(methyl methacrylate-co-*methacrylate isobutyl POSS) (PMMA*-co-*PMAPOSS) and Poly(methyl methacrylate*-co-*methacrylamide*-co-*methacrylate isobutyl-POSS) (PMMA*-co-*PMAAM*-co-*PAMPOSS) Copolymers*

The bulk copolymerization of MMA and MAPOSS monomers was in a beaker. The initiator BPO was added (ca. 1.5 wt% of monomers) were mixed at low temperature. After the mixture had dispersed, it was placed over a water bath at 60 °C for 12 h. The plates of the PMMA-*co*-PMAPOSS and PMMA-*co*-PMAAM-*co*-PMAPOSS copolymers were polymerized through a two-stage process. First, the polymerization stage was performed at 80 °C for 30 min; the second stage was bulk polymerization 60 °C for 24 hr. All experiments were conducted under atmospheric conditions. The resultant polymers were heated in an oven at 120 °C for 3 h to remove any unreacted monomers and initiator and maintain the stability of the copolymers.

2.2. Characterization

The thermal properties, including glass transition temperatures (T_g), of the copolymers were measured using a DSC Q100 instrument (TA Instruments) operated at a scan rate of 20 °C/min from 30 to 200 °C. Copolymers were weighed (ca. 5–7 mg) and sealed in an aluminum pan under an atmosphere of dry N_2. The decomposition temperatures (5% weight loss) of the copolymers were measured through TGA using a TA Q500 instrument. The copolymers (ca. 5–7 mg) were placed in a Pt cell. All TGA curves were measured at a scan rate of 20 °C/min from 30 to 800 °C under a N_2 atmosphere (60 mL/min). The dynamic mechanical property of PMMA copolymers were investigated by the Q800 dynamic mechanical analyzer. The PMMA copolymers were polished to ca. $2.0 \times 20.0 \times 10.0$ mm and then mounted on a single cantilever clamp. The mechanical properties were determined under the N_2 in step mode every 2 °C from 25 to 200 °C at 1 Hz frequency. Moisture absorption tests were conducted using the ASTM D570 standard method. The transmittance and yellow index were characterized using an NDH 2000 spectrophotometer (Nippon Denshoku Industries); the test film thickness was determined to be 5 mm. FTIR spectroscopic analyses of the copolymer compositions and specific interactions were performed using a Thermo Nicolet 380 ATR-FTIR spectrometer; the copolymers were prepared using the KBr disk method at room temperature; 32 scans were recorded at 4 cm^{-1} resolution. Molecular weights and molecular weight distributions (M_w/M_n) were measured through gel permeation chromatography (GPC). The system was equipped with three Ultrastyragel columns (100, 500, and 1000 Å) connected in series; dimethylformamide (DMF) was used as the eluent at a flow rate of 0.8 mL/min at 40 °C. Molecular weights were calibrated using PS standards and measured using light scattering and refractive index detectors. The water contact angles of the copolymers were measured at room temperature using an OPTIMA XE instrument (AST Products, Billerica, MA). Images of the film surfaces were recorded using a CCD camera; at least five measurements were averaged for each copolymer.

3. RESULTS AND DISCUSSION

To determine the effect of incorporating the bulky MAPOSS monomer into PMMA copolymers, we first

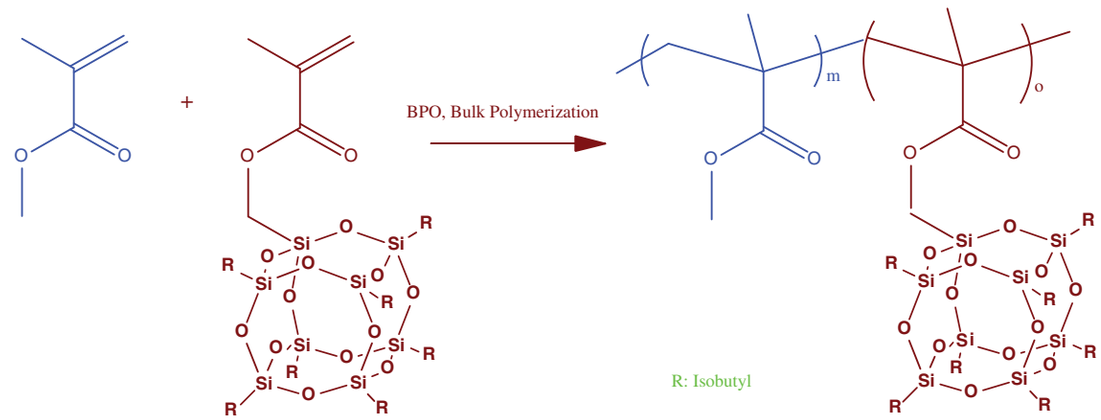

Scheme 1. Preparation of PMMA-*co*-PMAPOSS copolymers.

synthesized a series of PMMA-*co*-PMAPOSS random copolymers through free radical bulk copolymerization (Scheme 1). The copolymer compositions of these PMMA-*co*-PMAPOSS random copolymers were confirmed using FTIR spectroscopy (Fig. 1). Peaks appeared at 1724 and 1109 cm^{-1} for the carbonyl (C═O) and Si–O–Si stretching vibrations of the pure PMMA and PMAPOSS segments. The ratio of the signals at 1109 cm^{-1} (from the Si–O–Si units of PMAPOSS) to the signal at 1724 cm^{-1} (from the C═O units of both PMMA and PMAPOSS) increased upon increasing the PMAPOSS content in the PMMA-*co*-PMAPOSS random copolymers.

Figure 2 presents the second heating scans of DSC thermograms of pure PMMA and various PMMA-*co*-PMAPOSS random copolymers over the temperature range from 50 to 200 °C to avoid the thermal history problem. Pure PMMA displayed a value of T_g of 105°C; it increased to 123 °C at a low PMAPOSS content of 5 wt%, but decreased thereafter upon increasing the PMAPOSS content further in the PMMA-*co*-PMAPOSS random copolymers. The presence of pendant POSS nanoparticles in C═O copolymers usually has two effects: the inorganic POSS nanoparticles influence the thermal properties because of physical aggregation of

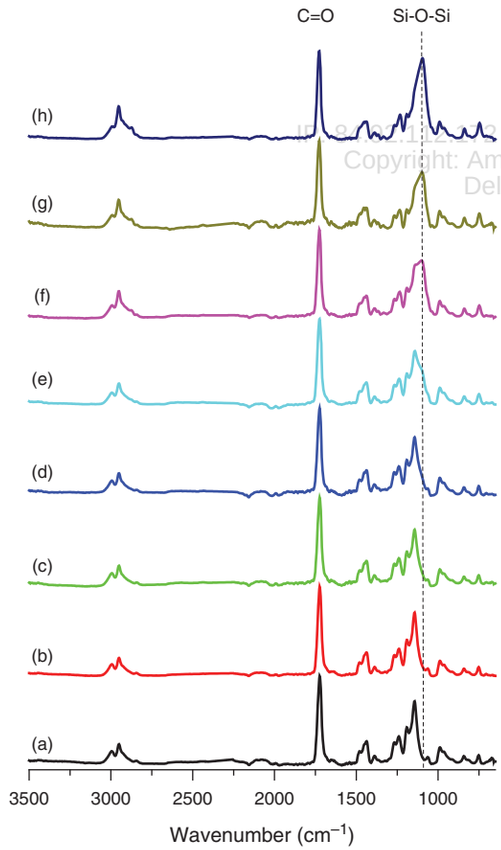

Figure 1. FTIR spectra of various PMMA-*co*-PMAPOSS copolymers recorded at room temperature: (a) pure PMMA, (b) PMMA-PMAPOSS1, (c) PMMA-PMAPOSS3, (d) PMMA-PMAPOSS5, (e) PMMA-MAPOSS10, (f) PMMA-PMAPOSS20, (g) PMMA-PMAPOSS25, and (h) PMMA-PMAPOSS30.

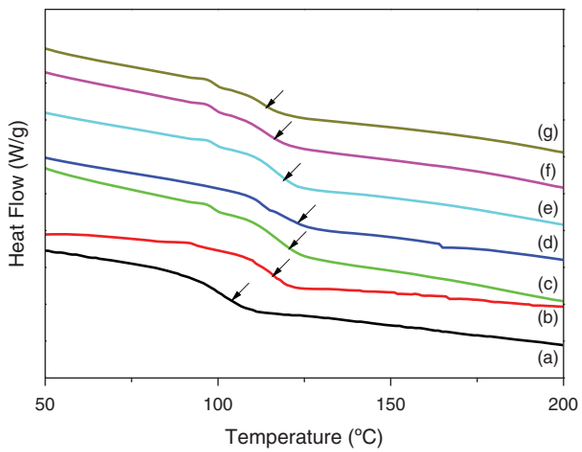

Figure 2. DSC thermograms of various PMMA-*co*-PMAPOSS copolymers: (a) pure PMMA, (b) PMMA-PMAPOSS1, (c) PMMA-PMAPOSS3, (d) PMMA-PMAPOSS5, (e) PMMA-MAPOSS10, (f) PMMA-PMAPOSS20, and (g) PMMA-PMAPOSS25.

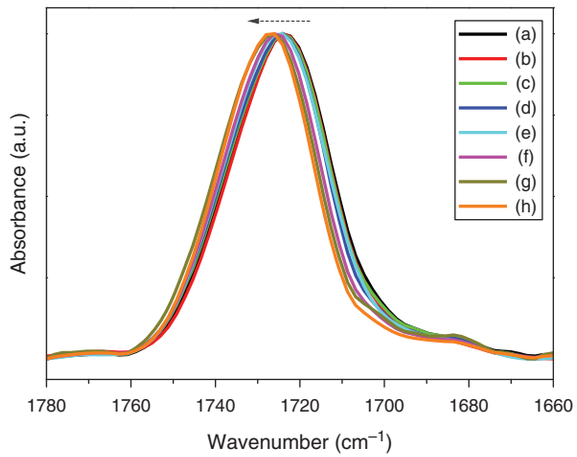

Figure 3. Scale-expanded (1780–1680 cm^{-1}) room-temperature FTIR spectra of (a) pure PMMA, (b) PMMA-PMAPOSS1, (c) PMMA-PMAPOSS3, (d) PMMA-PMAPOSS5, (e) PMMA-MAPOSS10, (f) PMMA-PMAPOSS20, (g) PMMA-PMAPOSS25, and (h) PMMA-PMAPOSS30.

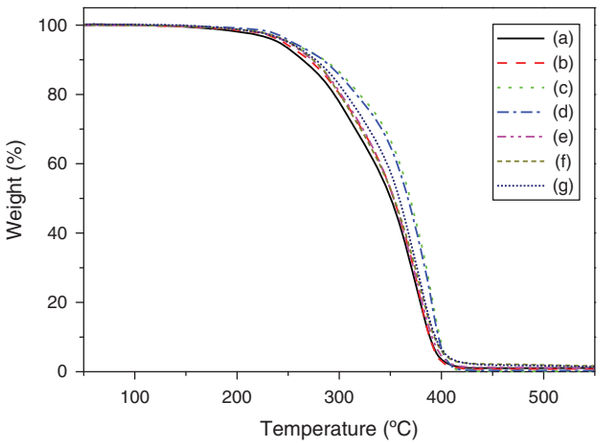

Figure 4. TGA curves of various PMMA-*co*-PMAPOSS copolymers: (a) pure PMMA, (b) PMMA-PMAPOSS1, (c) PMMA-PMAPOSS3, (d) PMMA-PMAPOSS5, (e) PMMA-PMAPOSS10, (f) PMMA-PMAPOSS20, and (g) PMMA-PMAPOSS25.

the nanosized POSS; and a diluent segment effect that weakens the dipole–dipole interactions among the PMMA segments.[28] Therefore, we believe that the values of T_g of the PMMA-*co*-PMAPOSS copolymer increased initially (to 123 °C) upon increasing the PMAPOSS content to 5 wt% because of physical aggregation of the nanosized POSS units. At higher PMAPOSS contents (>5 wt%), the values of T_g decreased upon increasing the PMAPOSS content in the PMMA-*co*-PMAPOSS random copolymers (e.g., $T_g = 114$ °C at 30 wt% PMAPOSS), due to the diluent segment effect of the POSS units weakening the dipole–dipole interactions of the PMMA segments.

To confirm weakening of the dipole–dipole interactions among the PMMA segments after the incorporation of PMAPOSS units, we used FTIR spectroscopy to investigate the specific interactions in these random copolymers. Figure 3 presents scale-expanded FTIR spectra (from 1780 to 1680 cm^{-1}) of the pure PMMA and various PMMA-*co*-PMAPOSS random copolymers, each recorded at room temperature. The absorption at 1724 cm^{-1} is assigned to the C═O groups of pure PMMA. The position of the signal for the C═O groups of PMMA shifted to higher wavenumber upon the incorporation of PMAPOSS units into the PMMA segments. This result is often observed for polymers containing C═O groups; for example, self-association arising from dipole–dipole interactions occurs for polyacetoxystyrene (PAS), polyvinylpyrrolidone, and poly(vinyl acetate) as a function of the concentration and strength of the dipoles.[30, 31] Generally, the density of polar C═O functional groups decreases after random copolymerization with inert diluent segments—for example, from copolymerization with styrene to form PS-*co*-PAS random copolymers or ethylene to form poly(ethylene-*co*-vinyl acetate) random copolymers.[31, 32] In this study, we observed that the signal of the C═O groups of PMMA shifted to higher wavenumber, indicating weaker self-association through dipole–dipole interactions, after the incorporation of the PMAPOSS segments; relatively high PMAPOSS contents led to lower glass transition temperatures of the PMMA-*co*-PMAPOSS random copolymers. The weaker dipole–dipole interactions after incorporating the PMAPOSS units into the PMMA copolymers affected not only the values of T_g (based on DSC analyses) but also the decomposition temperatures (T_d, based on TGA analyses), as revealed in Figure 4. The 5 wt% decomposition temperature for pure PMMA was approximately 310 °C; it increased to 346 °C at relatively low PMAPOSS contents (≤5 wt%), but decreased thereafter upon increasing the PMAPOSS content in the PMMA-*co*-PMAPOSS random copolymers. This behavior is similar to that in the DSC analyses. Table I summarizes the feed ratios, thermal properties, and molecular weights of the PMMA-*co*-PMAPOSS random copolymers used in this study. Based on the DSC results, we suggest that the 5 wt% PMAPOSS content provided the highest value of T_g because of a balance between the effects of physical aggregation of the POSS nanoparticles and the weaker dipole–dipole

Table I. Physical characteristics of the PMMA-*co*-PMAPOSS copolymers used in this study.

Polymer	Weight fraction MMA	Weight fraction MA-POSS	T_g (°C)	T_d (°C)	M_n (×10^4)	PDI
Pure PMMA	100	0	105	310	18.2	1.25
PMMA-PMAPOSS1	99	1	116	320	15.7	1.63
PMMA-PMAPOSS3	97	3	121	341	13.9	1.71
PMMA-PMAPOSS5	95	5	123	346	19.6	1.77
PMMA-PMAPOSS10	90	10	120	338	20.0	1.78
PMMA-PMAPOSS20	80	20	118	319	23.0	1.56
PMMA-PMAPOSS25	75	25	116	312	15.4	1.57
PMMA-PMAPOSS30	70	30	114	311	13.2	1.59

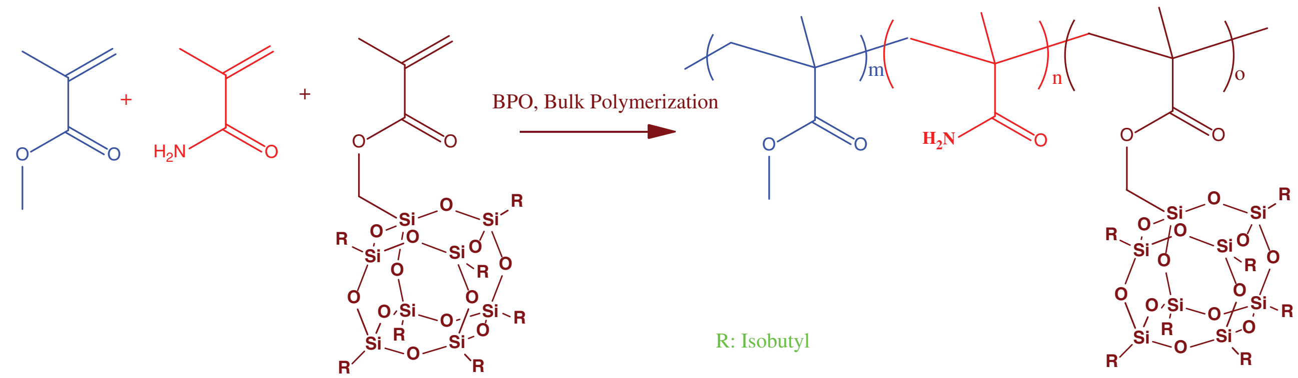

Scheme 2. Preparation of PMMA-*co*-PMAAM-*co*-PMAPOSS copolymers.

interactions. To further increase the glass transition temperature, we incorporated the strongly hydrogen bonding MAAM monomer units into the PMMA-*co*-PMAPOSS copolymers (Scheme 2, Table II).

Figure 5 displays scale-expanded (1800–1600 cm^{-1}) room-temperature FTIR spectra of pure PMMA, PMMA-*co*-PMAPOSS, and various PMMA-*co*-PMAAM-*co*-PMAPOSS random copolymers containing 5 wt% PMAPOSS. The signals at 1724 and 1680 cm^{-1} represent stretching of the C═O groups of the PMMA and PMAPOSS segments and the amide (CONH) groups of the PMAAM segments, respectively. The ratio of the signal at 1680 cm^{-1} (amide I absorption from PMAAM segments) increased upon increasing the PMAAM content in the PMMA-*co*-PMAAM-*co*-PMAPOSS random copolymers. Correspondingly, the signal of the C═O groups of PMMA shifted to slightly lower wavenumber, from 1724 to 1722 cm^{-1}, indicative of hydrogen bonding between the PMMA and PMAAM segments.

Figure 6 presents the corresponding second heating scans (from 50 to 200 °C) of DSC thermograms of various PMMA-*co*-PMAAM-*co*-PMAPOSS random copolymers

Table II. Physical characteristics of PMMA-*co*-PMAAM-*co*-PMAPOSS copolymers used in this study.

	Weight fraction					
Polymer	MMA	MAAM	MA-POSS	T_g (°C)	M_n ($\times 10^4$)	PDI
Pure PMMA	100	0	0	105	18.2	1.25
PMMA-PMAPOSS5	95	0	95	123	19.6	1.77
PMMA-PMAAM1-PMAPOSS5	94	1	5	125	30.2	1.74
PMMA-PMAAM3-PMAPOSS5	92	3	5	132	34.5	1.82
PMMA-PMAAM4-PMAPOSS5	91	4	5	139	60.5	1.58
PMMA-PMAAM5-PMAPOSS5	90	5	5	142	45.0	1.67
PMMA-PMAAM6-PMAPOSS5	89	6	5	139	43.1	1.75
PMMA-PMAAM7-PMAPOSS5	88	7	5	133	38.6	1.64

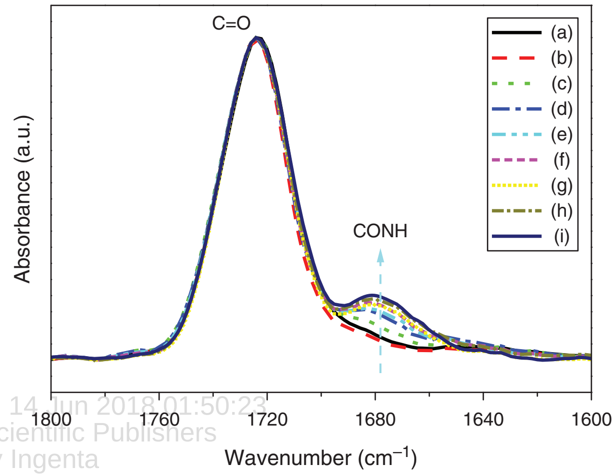

Figure 5. Scale-expanded (1800–1600 cm^{-1}) room-temperature FTIR spectra of (a) pure PMMA, (b) PMMA-PMAPOSS5, (c) PMMA-PMAAM1-PMAPOSS5, (d) PMMA-PMAAM2-MAPOSS5, (e) PMMA-PMAAM3-MAPOSS5, (f) PMMA-PMAAM4-PMAPOSS5, (g) PMMA-PMAAM5-PMAPOSS5, (h) PMMA-PMAAM6-PMAPOSS5, and (i) PMMA-PMAAM7-PMAPOSS5.

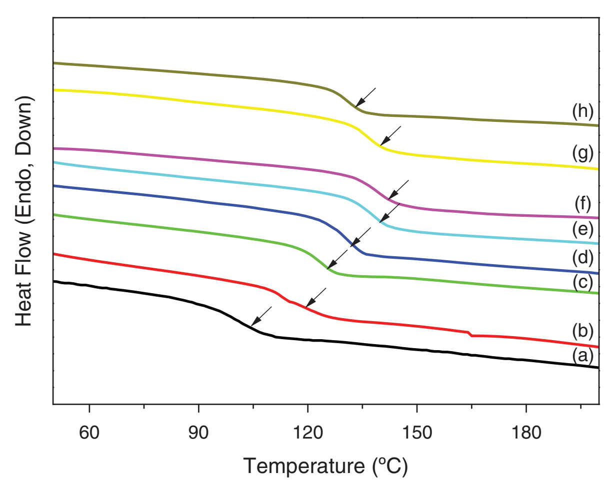

Figure 6. DSC thermograms of (a) pure PMMA, (b) PMMA-PMAPOSS5, (c) PMMA-PMAAM1-PMAPOSS5, (d) PMMA-PMAAM3-PMAPOSS5, (e) PMMA-PMAAM4-PMAPOSS5, (f) PMMA-PMAAM5-MAPOSS5, (g) PMMA-PMAAM6-PMAPOSS5, and (h) PMMA-PMAAM7-PMAPOSS5.

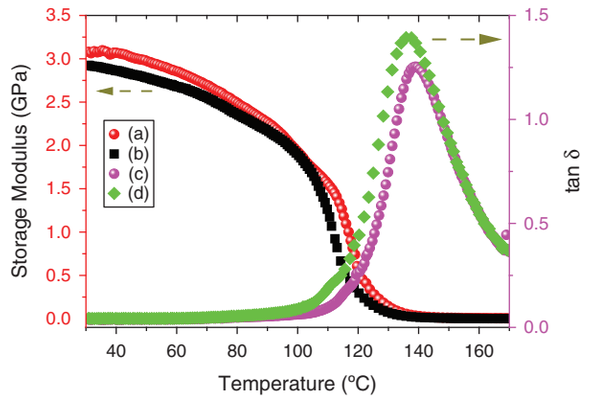

Figure 7. DMA analyses of the (a, b) storage modulus and (c, d) tan δ for (a, c) PMMA-PMAAM5-MAPOSS5 and (b, d) PMMA-PMAAM4-MAPOSS5.

containing 5 wt% PMAPOSS. Pure PMMA had a value of T_g of approximately 105 °C; it increased to 123 °C for the PMMA-*co*-PMAPOSS copolymer containing 5 wt% PMAPOSS. Incorporation of MAAM segments formed PMMA-*co*-PMAAM-*co*-PMAPOSS copolymers; the values of T_g increased initially to 142 °C at a 5 wt% PMAAM content and then decreased to 133 °C at 7 wt% PMAAM. We found that when the MAAM monomer content was greater than 6 wt%, it could not dissolve in the MMA monomer. This behavior may have been responsible for the poorer thermal properties of the PMMA-*co*-PMAAM-*co*-PMAPOS copolymers at higher PMAAM contents. As a result, the following discussion of the physical properties refers only to the effects of lower PMAAM contents in the PMMA-*co*-PMAAM-*co*-PMAPOS copolymers.

Figure 7 presents DMA thermograms of various PMMA-*co*-PMAAM-*co*-PMAPOSS random copolymers containing 5 wt% PMAPOSS. Contents of 5 wt% of both PMAAM and PMAPOSS units provided a value of T_g of approximately 141 °C, consistent with the behavior in the DSC analyses.[33] Both the values of T_g and the storage modulus were higher than those of the copolymer containing 4 wt% PMAAM and 5 wt% PMAPOSS units (T_g =138 °C), consistent with more hydrogen bonding units enhancing both the thermal and mechanical properties.

Figure 8 and Table II summarize the optical transparencies, water contact angles, and moisture absorption behavior of pure PMMA, PMMA-*co*-PMAAM random copolymers containing 4 and 5 wt% PMAAM, and PMMA-*co*-PMAAM-*co*-PMAPOSS random copolymers

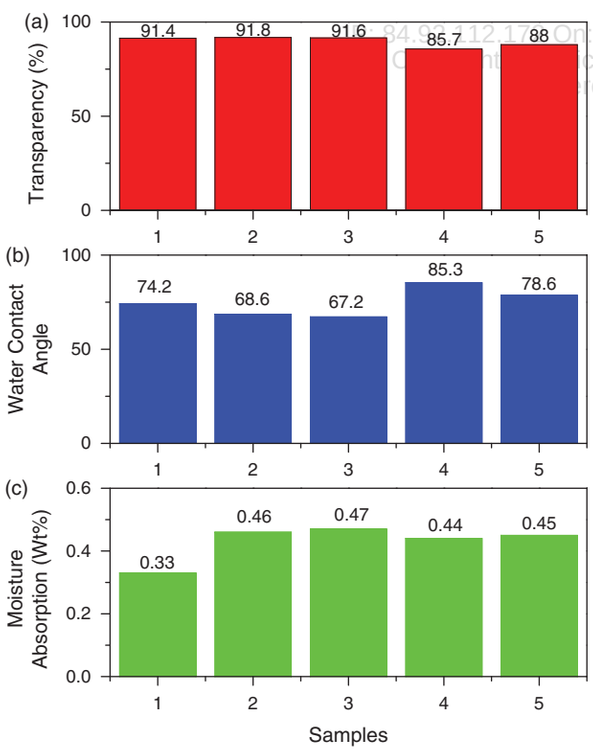

Figure 8. Optical transparency, water contact angle, and moisture absorption of (1) pure PMMA, (2, 3) PMMA-*co*-PMAAM random copolymers containing (2) 4 and (3) 5 wt% PMAAM, and (4, 5) PMMA-*co*-PMAAM-*co*-PMAPOSS random copolymers containing 5 wt% PMAPOSS and (4) 4 and (5) 5 wt% PMAAM.

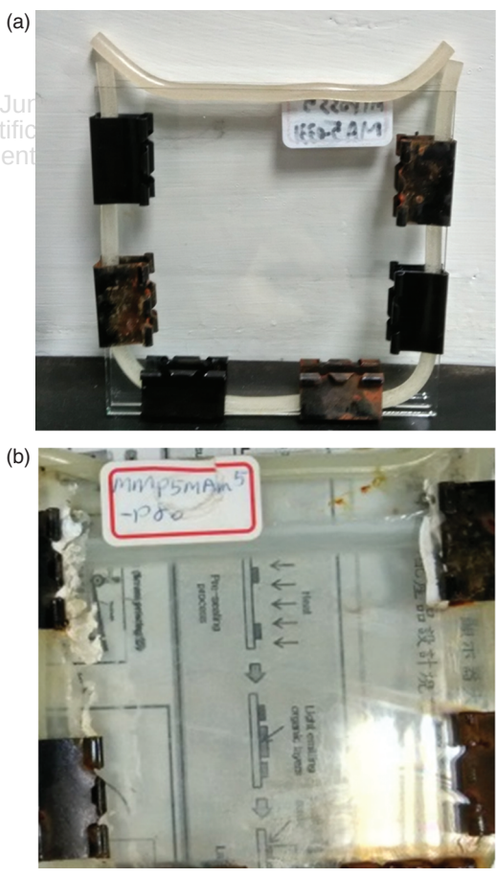

Figure 9. The photography of (a) mold and (b) the bulk PMMA-*co*-PMAAM5-*co*-PMAPOSS random copolymer displayed high transparency.

containing 4 and 5 wt% PMAAM and 5 wt% PMAPOSS. The pure PMMA and the two PMMA-*co*-PMAAM random copolymers displayed relatively higher transparency (>90%). Although the transparency decreased after incorporating PMAPOSS units into the PMMA-*co*-PMAAM random copolymer, it remained at approximately 85–88%. The bulk PMMA-*co*-PMAAM5-*co*-PMAPOSS random copolymer displayed high transparency (Fig. 9). The water contact angles decreased and the degrees of moisture absorption increased after copolymerizing MMA with MAAM, suggesting that PMMA-*co*-PMAAM became hydrophilic because of hydrogen bonding in PMMA/PMAAM segments. Nevertheless, further copolymerization with MAPOSS caused the water contact angle to increase and the degree of moisture absorption to decrease, suggesting that the PMMA-*co*-PMAAM-*co*-PMAPOSS copolymers became more hydrophobic.

4. CONCLUSIONS

A series of PMMA-*co*-PMAAM-*co*-PMAPOSS random copolymers containing low amounts of MAAM and MAPOSS monomer units have been prepared through bulk polymerization. The incorporation of the bulky POSS monomer maintained PMMA's excellent transmittance in the near-UV region and lower moisture absorption, while the hydrogen bonding of the MAAM monomer units hindered the free rotation of the PMMA copolymers and, thereby, enhanced the thermal properties. The PMMA copolymer incorporating 5 wt% PMAAM and 5 wt% PMAPOSS displayed an enhanced value of T_g (to 142 °C), a higher modulus, a higher water contact angle, and reasonable high transparency. Accordingly, such copolymers have potential uses in optical applications as replacements for PMMA homopolymers.

Acknowledgment: This study was supported financially by the Ministry of Science and Technology, Taiwan, Republic of China, under contracts MOST103-2221-E-110-079-MY3 and MOST105-2221-E-110-092-MY3.

References and Notes

1. C. D. Entwistle and T. B. Marder, *Chem. Mater.* 16, 4574 (**2004**).
2. H. K. Shih, Y. H. Chen, Y. L. Chu, C. C. Cheng, F. C. Chang, C. Y. Zhu, and S. W. Kuo, *Polymers* 7, 804 (**2015**).
3. G. A. Kim, *Eur. Polym. J.* 41, 1729 (**2005**).
4. Y. Kita, K. Kishino, and K. Nakagawa, *J. Appl. Polym. Sci.* 63, 363 (**1997**).
5. V. G. Syronmyatnikov, L. P. Paskal, and I. A. Savchenko, *Russ. Chem. Rev*. 68, 781 (**1999**).
6. H. Teng, K. Koike, D. Zhou, Z. Satoh, Y. Koike, and Y. Okamoto, *J. Polym. Sci. Part A: Polym. Chem.* 47, 315 (**2009**).
7. A. Mishra, T. M. J. Sinha, and V. Choudhary, *J. Appl. Polym. Sci.* 68, 527 (**1998**).
8. S. Dong, Q. Wang, Y. Wei, and Z. Zhang, *J. Appl. Polym. Sci.,* 72, 1335 (**1999**).
9. A. Tagaya, T. Harada, K. Koike, Y. Koike, Y. Okamoto, H. Teng, and L. Yang, *J. Appl. Polym. Sci.* 106, 4219 (**2007**).
10. S. W. Kuo and H. T. Tsai, *Appl. Polym. Sci.* 123, 3275 (**2012**).
11. B. Tang, C. Wu, T. Lin, and S. Zhang, *Dyes Pigments* 99, 1022 (**2013**).
12. D. J. Wang, C. B. Gu, P. L. Chen, S. X. Liu, Z. Zhen, J. C. Zhang, and X. H. Liu, *J. Appl. Polym. Sci.* 87, 280 (**2003**).
13. M. Teresa, R. Luguna, J. Gallego, F. Mendicuti, E. Saiz, and M. P. Tarazona, *Macromolecules* 35, 7782 (**2002**).
14. A. Takasu, H. Yamamoto, Y. Inai, T. Hirabayashi, K. Nagata, and K. Takahashi, *Macromolecules* 34, 6235 (**2001**).
15. A. Matsumoto, K. Mizuta, and T. Otsu, *Macromolecules* 26, 1659 (**1993**).
16. P. P. Wu, D. M. Zhao, L. X. Li, H. S. Wang, and G. D. Liu, *Polym. Eng. Sci.* 53, 2370 (**2013**).
17. S. W. Kuo, H. C. Kao, and F. C. Chang, *Polymer* 44, 6873 (**2003**).
18. J. K. Chen, S. W. Kuo, H. C. Kao, and F. C. Chang, *Polymer* 46, 2354 (**2005**).
19. S. W. Kuo and H. T. Tsai, *Macromolecules* 42, 4701 (**2009**).
20. C. T. Lin, S. W. Kuo, C. F. Huang, and F. C. Chang, *Polymer* 51, 883 (**2010**).
21. S. L. Yeh, C. Y. Zhu, and S. W. Kuo, *Polymers* 7, 1379 (**2015**).
22. M. M. Coleman, Y. Xu, and P. C. Painter, *Macromolecules* 27, 127 (**1994**).
23. M. Aono and K. Ariga, *Adv. Mater.* 28, 989 (**2016**).
24. K. Ariga, K. Minami, M. Ebara, and J. Nakanishi, *Polym. J.* 48, 371 (**2016**).
25. K. Ariga, Q. Ji, W. Nakanishi, J. P. Hill, and M. Aono, *Mater. Horz.* 2, 406 (**2015**).
26. C. H. Wanke, D. Pozzo, C. Luvison, I. Krindges, C, Aguzzoli, M. R. F. Soares, and O. Bianchi, *Polym. Testing* 54, 214 (**2016**).
27. S. W. Kuo and F. C. Chang, *Prog. Polym. Sci.* 36, 1649 (**2011**).
28. M. G. Mohamed and S. W. Kuo, *Polymers* 8, 225 (**2016**).
29. C. W. Chiou, Y. C. Lin, L. Wang, C. Hirano, Y. Suzuki, T. Hayakawa, and S. W. Kuo, *Polymers* 6, 926 (**2014**).
30. H. Y. Xu, S. W. Kuo, J. S. Lee, and F. C. Chang, *Macromolecules* 35, 8788 (**2002**).
31. S. W. Kuo, W. J. Huang, C. F. Huang, S. C. Chan, and F. C. Chang, *Macromolecules* 37, 4164 (**2004**).
32. Y. Hu, H. R. Motzer, A. M. Etxeberria, M. J. Fernandez-Berridi, J. J. Iruin, P. C. Painter, and M. M. Coleman, *Macromol. Chem. Phys.* 201, 705 (**2000**).
33. I. Blanco, I. L. Abate, F. A. Bottino, and P. Bottion, *Polym. Degrad. Stab.* 97, 849 (**2012**).

Received: 14 November 2016. Accepted: 28 November 2016.